Microstructural evolution and enhanced superplasticity in friction stir processed Mg–Zn–Y–Zr alloy

G.M. Xie
Shenyang National Laboratory for Materials Science, Institute of Metal Research, Chinese Academy of Sciences, Shenyang 110016, People's Republic of China; and School of Materials Science and Engineering, Harbin Institute of Technology, Harbin 150001, People's Republic of China

Z.Y. Ma[a)]
Shenyang National Laboratory for Materials Science, Institute of Metal Research, Chinese Academy of Sciences, Shenyang 110016, People's Republic of China

L. Geng
School of Materials Science and Engineering, Harbin Institute of Technology, Harbin 150001, People's Republic of China

R.S. Chen
Shenyang National Laboratory for Materials Science, Institute of Metal Research, Chinese Academy of Sciences, Shenyang 110016, People's Republic of China

(Received 20 July 2007; accepted 8 October 2007)

The extruded Mg–Zn–Y–Zr plate was subjected to friction stir processing (FSP). FSP resulted in significant breakup and dispersion of bulky W-phase particles and remarkable grain refinement, thereby substantially enhancing superplasticity. Maximum superplasticity of 635% was achieved at 450 °C and a relatively high strain rate of 3×10^{-3} s^{-1}. By comparison, the as-extruded sample did not exhibit superplasticity. Grain boundary sliding was identified to be the primary deformation mechanism in the FSP Mg–Zn–Y–Zr by superplastic data analyses and surfacial morphology observations. Furthermore, the superplastic deformation kinetics of the FSP Mg–Zn–Y–Zr is significantly faster than that of equal channel angular pressed (ECAP) magnesium alloys under both as-ECAP and annealing conditions.

I. INTRODUCTION

There is significant interest in the development of wrought magnesium alloys with high strength and high corrosion resistance for application as structural parts. To achieve high strength in magnesium alloys, the alloys must undergo dynamic recrystallization (DRX) during hot processing, yielding a fine-grained microstructure. For conventional AZ (Mg–Al–Zn) system alloys containing $Mg_{17}Al_{12}$ particles, the particles have poor thermal stability during hot deformation due to the low solution temperature of particles, easily resulting in grain growth and cavitation.[1] Mg–Zn–Y–Zr is a heat-resistant magnesium alloy with high strength. There are mainly two kinds of ternary phases in the Mg–Zn–Y system, i.e., the I-phase (quasicrystal phase, Mg_3Zn_6Y) and the W-phase ($Mg_3Zn_3Y_2$), and their eutectic temperatures are ~450 and 510 °C, respectively.[2] Because of the existence of the high melting point phases and the Zr element, the Mg–Zn–Y–Zr alloy exhibits a sound high temperature-resistant capability and high strength. Therefore, the Mg–Zn–Y–Zr alloy has important application potential for wrought magnesium alloys. Recently, several superplastic investigations were focused on the Mg–Zn–Y–Zr alloy containing only the I-phase. Superplasticity has been achieved in this alloy prepared by using hot rolling, hot extrusion, and equal channel angular pressing (ECAP).[3,4] However, the optimum strain rate for superplasticity was generally at a lower strain rate of ~10^{-4} s^{-1}.

Friction stir welding (FSW) is a simple, clean, and innovative joining technology invented by The Welding Institute of the UK in 1991.[5] Friction stir processing (FSP), a new solid-state processing technique, has been developed based on the basic principles of FSW.[6] FSP results in the generation of fine recrystallized grains with dominant high-angle boundaries, thereby enhancing the superplasticity of the processed zone significantly.[7] Currently, superplasticity via FSP is mainly focused on aluminum alloys,[7,8] and there are few superplastic investigations on FSP magnesium alloys. Cavaliere et al.

a)Address all correspondence to this author.
e-mail: zyma@imr.ac.cn
DOI: 10.1557/JMR.2008.0164

reported that for AZ91 and AM60, good superplasticity was achieved via FSP with an optimum strain rate of 10^{-4} to 10^{-3} s^{-1}.[9,10] However, they did not analyze the superplastic data in detail and compare their data to those of the magnesium alloys prepared by other severe plastic deformation methods.

In our previous work, FSW of Mg–Zn–Y–Zr alloy containing both the I-phase and the W-phase has been reported. It was indicated that FSW resulted in the effective refinement of the bulky ternary phases and coarse grains, thereby generating sound joints with good mechanical properties.[2] Because the eutectic temperature (510 °C) of the W-phase is higher than that (450 °C) of the I-phase, the Mg–Zn–Y–Zr alloy containing the W-phase would have higher thermal stability than that containing only the I-phase. Therefore, it is expected that the superplasticity could be achieved at a higher temperature and consequently at a higher strain rate. In the present work, a Mg–Zn–Y–Zr alloy containing only the W-phase was subjected to FSP to examine the possibility of achieving superplasticity at a higher temperature and a higher strain rate. Further, the superplastic deformation mechanism of the FSP Mg–Zn–Y–Zr was examined and analyzed in detail.

II. EXPERIMENTAL

The extruded Mg–Zn–Y–Zr alloy plate (extruded ratio is 25:1) with a composition of 6.19Zn–1.1Y–0.46Zr (in wt%) was used for this study. The 6-mm-thick, 100-mm-long, and 50-mm-wide plates were machined from the extruded plate and subjected to FSP at a tool rotation rate of 800 rpm and a traverse speed of 100 mm/min by using a gantry FSW machine (China FSW Center, Beijing, China). A tool with a shoulder 20 mm in diameter and a coniform threaded pin 6 mm in diameter and 5.7 mm in length was used. The tilting angle for the FSP was maintained at 2.5°. Before FSP, the plates were cleared with a wire brush to remove the surface oxide layer.

The FSP samples were cross-sectioned perpendicular to the processing direction, polished, and then etched with a solution of 90 mL ethanol, 10 mL distilled water, 5 mL acetic acid, and 5 g picric acid. Microstructural features were characterized by optical microscopy (OM) and scanning electron microscopy (SEM). Grain size was measured by the mean linear intercept method. Composition of phase in the parent material (PM) and FSP sample were analyzed by a Philips type x-ray diffractometer. To investigate thermal stability of the W-phase in the Mg–Zn–Y–Zr alloy, differential scanning calorimetry (DSC) was conducted at a heating rate of 10 °C/min.

To evaluate the superplasticity of the FSP sample, tensile specimens with 2.5 mm gauge length and 1.4 mm width were machined from the processed zone perpendicular to the FSP direction. For comparison, tensile specimens of the PM were machined with the same specimen configuration parallel and perpendicular to the extruded direction, respectively (hereafter referred to as PM-L and PM-T). Constant crosshead speed tensile tests were performed using an Instron (Norwood, MA) 5848 micro-tester at 400–450 °C for initial strain rates of 3×10^{-4} to 1×10^{-2} s^{-1}. All tensile specimens were held at the required temperature for 15 min prior to loading. The failed specimens with or without polishing were subjected to OM and SEM examinations.

III. RESULTS

Figure 1 shows the macrostructures of the FSP Mg–Zn–Y–Zr. The processed zone is clearly visible with distinct boundaries on both the advancing and retreating sides. Neither crack nor porosity was found in the processed zone, indicating good processing quality. The microstructures of the PM and the processed zone (hereafter referred to as FSP sample) are shown in Fig. 2. The PM was characterized by coarse grains and large heterogeneously distributed second phase particles [Figs. 2(a) and 2(c)]. After FSP, a fine-grained structure of 5.2 μm with homogeneously-distributed second phase particles was produced in the FSP sample [Figs. 2(b) and 2(d)]. The size of both the grains and second phase particles in the FSP sample was significantly smaller than that in the PM.

Figure 3 shows the x-ray diffraction (XRD) patterns of the PM and FSP sample. For the PM, the diffraction peaks of the a-Mg, W-phase, and MgZn were detected, and no diffraction peak of the I-phase was found. After FSP, the diffraction peaks of the W-phase remained, but the diffraction peaks of the MgZn phase disappeared fundamentally. Figure 4 shows DSC results of the PM and FSP sample. Only one endothermic peak was observed at 517 and 510 °C for the PM and FSP sample, respectively. Based on our previous work[2] and XRD analysis, both endothermic peaks correspond to the dissolution of the W-phase.

Figure 5 shows the effect of the initial strain rate and temperature on superplastic ductility of the FSP Mg–Zn–Y–Zr alloy. For the FSP sample, an optimum strain rate of 1×10^{-3} s^{-1} for maximum elongation was observed at 400 and 425 °C. However, at 450 °C, the optimum strain rate for maximum superplasticity was shifted to a higher

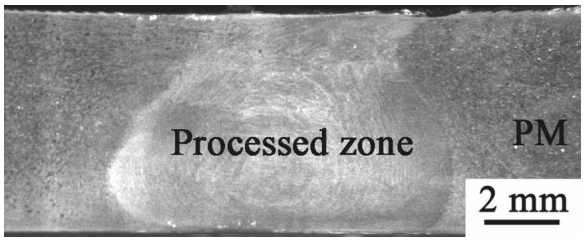

FIG. 1. Cross-sectional macrograph of FSP specimen.

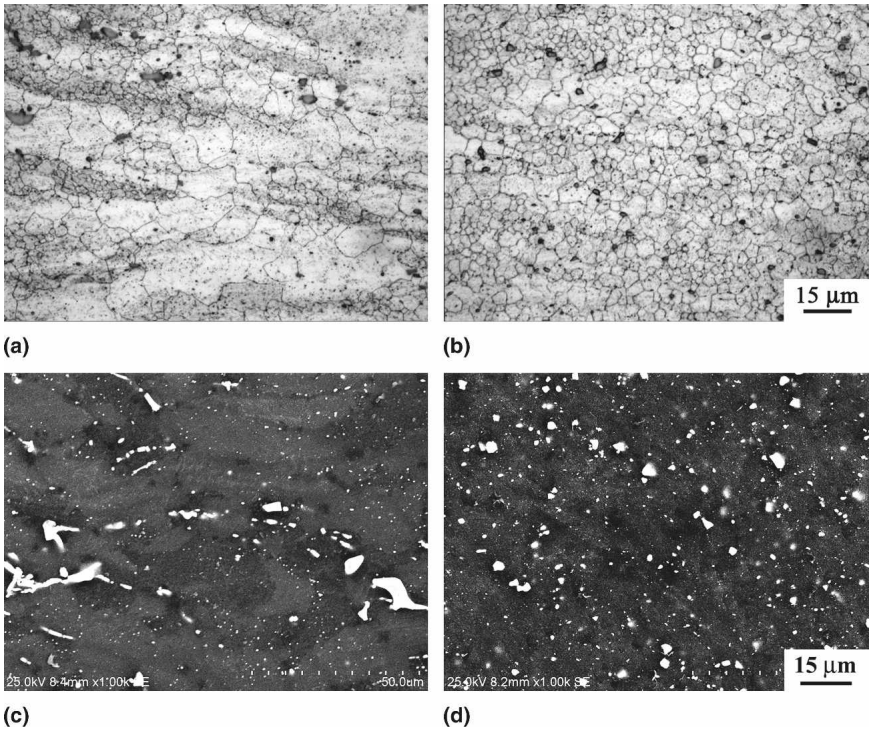

FIG. 2. OM and SEM micrographs showing (a, b) grain structure (OM), (c, d) W-phase particle distribution (SEM) in the Mg–Zn–Y–Zr alloy: (a, c) extruded PM and (b, d) FSP sample (extrusion/FSP directions are perpendicular to page).

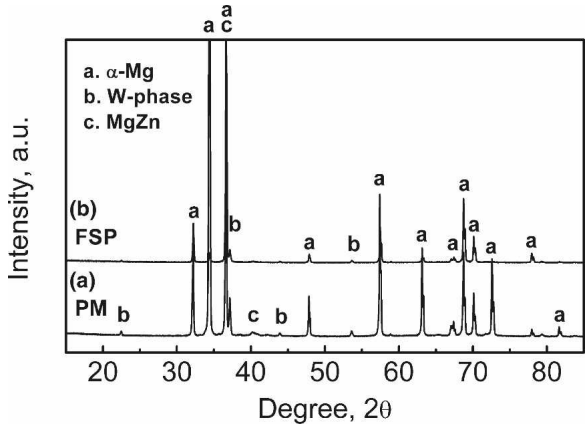

FIG. 3. XRD patterns of Mg–Zn–Y–Zr alloy: (a) PM sample and (b) FSP sample.

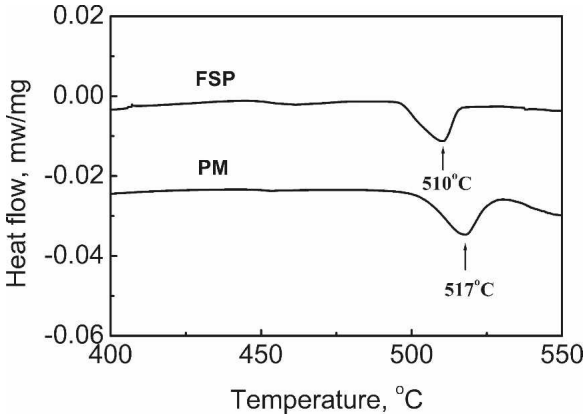

FIG. 4. DSC curves of Mg–Zn–Y–Zr alloy.

value of 3×10^{-3} s^{-1}. Maximum elongation of 635% was achieved at a relatively high strain rate of 3×10^{-3} s^{-1} and 450 °C [Fig. 5(a)]. By comparison, the PM did not exhibit superplasticity at 450 °C except for a strain rate of 3×10^{-4} s^{-1}, where the PM exhibited an elongation of 280% along the transverse direction. At an initial strain rate of 3×10^{-3} s^{-1}, the FSP sample exhibited an increasing elongation with increasing temperature from 375 to 450 °C, whereas above 450 °C, the elongation of the FSP sample decreased rapidly [Fig. 5(b)].

Figure 6 shows the variation of flow stress with initial strain rate for the FSP sample and PM. The flow stress of the FSP sample is significantly lower than that of the extruded PM at the initial strain rates of 3×10^{-4} to 1×10^{-2} s^{-1}. This is attributed to a significantly refined microstructure. The strain rate sensitivity m of the PM along both the longitudinal and transverse directions was consistently ~0.2 throughout the investigated strain rates of 3×10^{-4} to 1×10^{-2} s^{-1}. By comparison, the strain rate sensitivity of the FSP sample was ~0.5 within the investigated strain rates of 3×10^{-4} to 1×10^{-2} s^{-1}.

Figure 7 displays the untested and tested tensile specimens for the FSP Mg–Zn–Y–Zr alloy deformed to failure at 450 °C for different strain rates. The specimens show

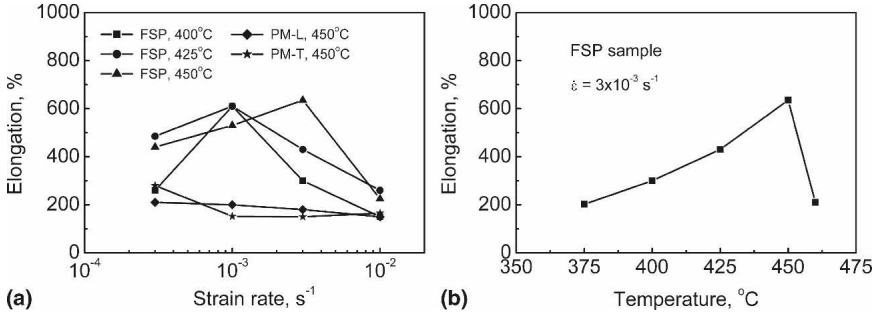

FIG. 5. Variation of elongation with (a) initial strain rate and (b) testing temperature for FSP Mg–Zn–Y–Zr alloy.

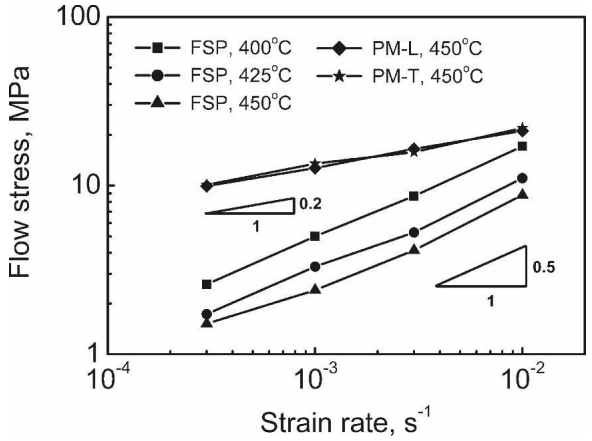

FIG. 6. Variation of flow stress with initial strain rate for FSP Mg–Zn–Y–Zr and PM.

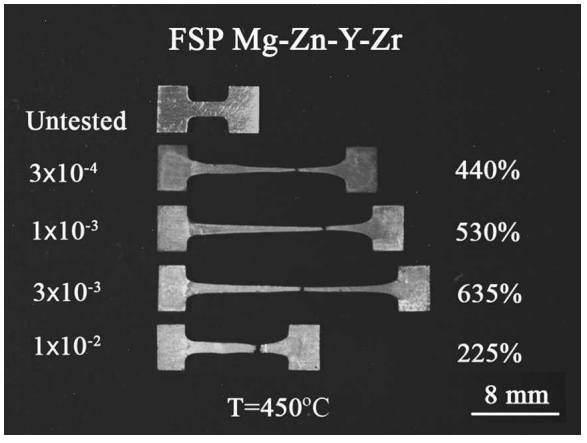

FIG. 7. Appearance of specimens before and after superplastic deformation at 450 °C for different initial strain rates.

neck-free elongation, which is characteristic of superplastic flow.

IV. DISCUSSION

It is widely accepted that FSP causes intense plastic deformation and thermal exposure in the processed zone, thereby resulting in the breaking of initial structure, mixing of material, and occurrence of dynamic recrystallization.[6] Therefore, the remarkable microstructural refinement and homogenization in the FSP Mg–Zn–Y–Zr are attributed to significant breaking and dispersion effect of the threaded pin and the dynamic recrystallization. Similarly, a previous study has indicated that FSW resulted in significant breakup and dispersion of both I-phase and W-phase particles in a Mg–6%Zn–0.6Y–0.6Zr alloy.[2] It should be pointed out that the grain size of this FSP Mg–Zn–Y–Zr was significantly smaller than that of the FSP AD91D and the FSW AM60 and AZ61.[11–13] This is attributed to the obvious grain refinement effect resulting from the zirconium element. Similar observations have been made in an FSW ZK60 alloy.[14]

In the past few years, several studies have been conducted to understand the effect of the Y content and Zn/Y ratio on the types of the Mg–Zn–Y ternary phases. In Mg–5.4Zn–(0.7–1.7)Y–0.4Zr (in wt%) alloys, Zhang et al.[15] reported that with a Y content of ⩽1.35 wt%, the alloy consisted of the a-Mg and I-phase, whereas for a higher Y content of 1.7 wt%, the W-phase appeared. On the other hand, Lee et al.[16] reported that in as-cast Mg–Zn–Y alloys, the ternary phase was the I-phase for a Zn/Y ratio of 5–7 (Y content: 0.5–1.6 wt%), the I-phase and W-phase for a Zn/Y ratio of 2–2.5 (Y content: 1.2–2.5 wt%), and the W-phase for a Zn/Y ratio of 1.5–2.0. Similarly, Kim and Bae[3] and Zheng et al.[4] reported that the I-phase was the main ternary phase in Mg–3.0Zn–0.5Y–1.5Zr and Mg–4.3Zn–0.7Y (in wt%). However, for the present Mg–Zn–Y–Zr alloy with a Y content of 1.1 wt% and a Zn/Y ratio of 5.6, the W-phase was identified to be the only ternary phase by the XRD pattern (Fig. 3). This observation is not consistent with that in Refs. 15 and 16, indicating that the factors influencing the formation of the ternary eutectic phases in the Mg–Zn–Y–Zr alloys are quite complicated.

The DSC analysis indicates that the dissolution of the W-phase occurred at 517 and 510 °C for the PM and FSP samples, respectively (Fig. 4). Clearly, the W-phase is thermally stable below ~500 °C. The XRD patterns indicate that the MgZn phase was fundamentally dissolved and the W-phase remained after FSP. The dissolution of the MgZn phase was previously observed in FSW Mg–6Zn–0.6Y–0.6Zr alloy.[2] This indicates that the

temperature rise during FSP was higher than the dissolution temperature (340 °C) of the MgZn phase but lower than the eutectic temperature (510 °C) of the W-phase. Therefore, the W-phase was thermally stable during the FSP thermal cycle.

For AZ91, AM60, and ZK60, superplasticity is usually achieved at low temperatures ≤350 °C due to poor thermal stability resulting from the absence of the pinning particles. Thus, the optimum strain rate for maximum elongation is usually within the lower strain rate range of 10^{-4} to 10^{-3} s^{-1}.[9,10,17] It is generally accepted that the addition of the Zr element into the Mg–Zn–Y alloy does not change the eutectic temperature of the I-phase.[15,18] Therefore, for Mg–Zn–Y–Zr alloy containing only the I-phase, a good superplasticity was hardly able to be achieved at higher temperatures due to the relatively low eutectic temperature (450 °C) of the I-phase. For example, Zheng et al. reported that ECAP Mg–4.3Zn–0.7Y alloy containing the I-phase exhibited a maximum elongation of ~600% at 350 °C and a initial strain rate of 1.5×10^{-4} s^{-1}.[4] However, Kim and Bae reported that for hot-rolled Mg–3.0Zn–0.5Y–1.5Zr alloy containing only the I-phase, a maximum elongation of 600% was observed at 450 °C and 5×10^{-4} s^{-1}.[3] They suggested that the addition of the Zr element increased the lattice constant of the I-phase to 5.49 Å, and therefore, the eutectic temperature of the I-phase was raised to 500 °C.[3]

Clearly, the existence of the heat-resistant (~500 °C) pinning particles is a prerequisite for achieving superplasticity at higher temperatures of up to 450 °C in the magnesium alloys. However, when the testing temperature is higher than 450 °C, superplasticity of the FSP Mg–Zn–Y–Zr decreased drastically. An examination on a polished specimen deformed at 460 °C and 3×10^{-3} s^{-1} revealed remarkable coarsening of the grains [Figs. 2(b) and 8], which decreased the superplasticity of the FSP sample significantly. To increase the thermal stability of the FSP sample for superplasticity at higher temperatures and consequently at higher strain rates (≥1×10^{-2} s^{-1}), it is necessary to reduce the size of the W-phase particles further. Furthermore, the decrease in the size of second phase particles also contributes to enhancing superplasticity because the particles are preferential nucleation sites for superplastic cavities, and small particles reduce cavitation level significantly.[19,20] A study for optimizing the FSP parameters is under progress to reduce the W-phase particle size and improve the particle distribution to enhance the superplasticity and increase the strain rate to a higher value (≥1×10^{-2} s^{-1}).

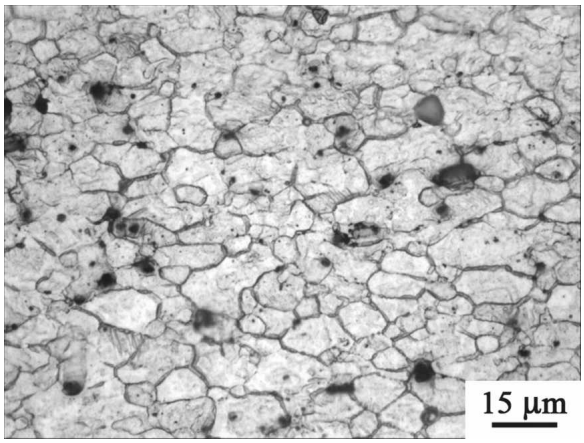

FIG. 8. Optical micrograph showing significant grain growth in gage length of FSP Mg–Zn–Y–Zr superplastically deformed at 450 °C with 3×10^{-3} s^{-1} (etched).

It is important to note that although the same optimum temperature of 450 °C was observed in Ref. 3 and in this study, the optimum strain rate in this study is nearly one order of magnitude higher than that in Ref. 3. This is attributed to different grain boundary characteristics. Usually, there is a great amount of non-equilibrium grain boundaries in metallic alloys processed by extrusion, rolling, and ECAP.[21] Mabuchi et al.[21] pointed out that the existence of the non-equilibrium grain boundaries in ECAP magnesium alloys retards the superplasticity strain rate. By comparison, the FSP alloys have a complete recrystallized microstructure with a higher ratio of high-angle boundaries (85%–95%),[22–24] and this ratio is much larger than that obtained with conventional thermal working techniques.[8] Therefore, this FSP Mg–Zn–Y–Zr alloy exhibited increased optimum superplasticity strain rate. This will be further discussed later.

For the as-extruded Mg–Zn–Y–Zr alloy, a low strain rate sensitivity of ~0.2 throughout the investigated strain rates of 3×10^{-4} to 1×10^{-2} s^{-1} accounts for the absence of superplasticity in the extruded PM. This is attributed to the coarse grains and the existence of coarse and heterogeneously-distributed W-phase particles. For the FSP Mg–Zn–Y–Zr alloy, the m value of 0.5 justifies the generation of superplasticity and suggests that the grain boundary sliding (GBS) is the main deformation mechanism.[25] This suggestion was supported by the SEM examinations on the surface of the tensile specimen deformed at 450 °C and 3×10^{-3} s^{-1} to failure. The evidence of extensive GBS was revealed (Fig. 9).

Recently, Cavaliere and Marco investigated the superplastic behavior of FSP fine-grained AZ91 and AM60 alloys at 175–300 °C and the strain rates of 1×10^{-4} to 1×10^{-2} s^{-1}.[9,10] Excellent superplasticity of more than 1000% was observed at the strain rates of 1×10^{-4} to 1×10^{-3} s^{-1}. Further, sigmoidal flow stress–strain rate curves were observed with a high strain rate sensitivity of ~0.7 at the strain rates of 1×10^{-4} to 1×10^{-3} s^{-1}. The observation in Refs. 9 and 10 is quite different from that in this study where an m value of ~0.5 was observed within the investigated strain rates of 3×10^{-4} to 1×10^{-2} s^{-1}. Although grain boundary sliding was revealed on the surface of deformed specimens, the

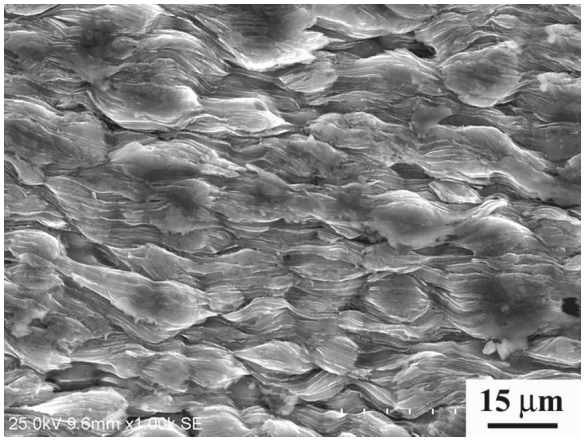

FIG. 9. SEM micrograph showing grain boundary sliding in gage length surface of FSP Mg–Zn–Y–Zr superplastically deformed at 450 °C with 3×10^{-3} s^{-1}.

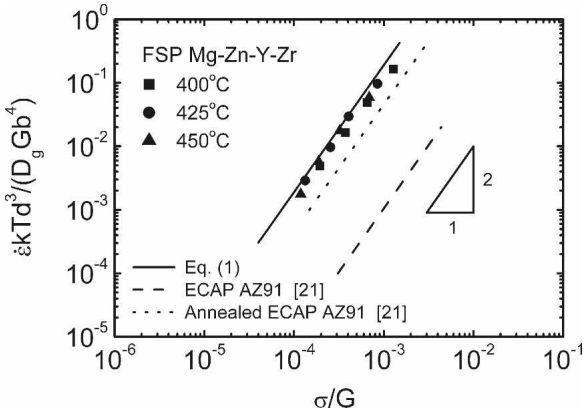

FIG. 10. Variation of $\dot{\epsilon}kTd^3/D_gGb^4$ with normalized effective stress, σ/G, for FSP Mg–Zn–Y–Zr alloy.

superplastic data of the FSP AZ91 and AM60 alloys were not analyzed and compared to those of magnesium alloys processed by other working techniques.[9,10] In previous studies, it was reported that FSP fine-grained aluminum alloys exhibited significantly enhanced superplastic deformation kinetics.[7,8] This has been attributed to a higher ratio of high-angle boundaries (85%–95%) in the FSP/FSW aluminum alloys.[8,22–24] Therefore, it is worthwhile to compare the superplastic data of the FSP Mg–Zn–Y–Zr alloy to the prediction by the constitutive equation for superplasticity in fine-grained magnesium alloys, as well as those of magnesium alloys prepared by other processing techniques, such as ECAP.

Watanabe et al. have analyzed superplastic data for a number of powder metallurgy magnesium alloys and extruded magnesium alloys with subsequent annealing.[26] They suggested that the superplastic deformation behavior of fine-grained (<10 μm) magnesium alloys with the GBS as main deformation mechanism can be described by a constitutive equation[26]:

$$\dot{\epsilon} = 2 \times 10^5 \left(\frac{D_0 Gb}{kT}\right) \exp\left(-\frac{92\ 000}{RT}\right)\left(\frac{b}{d}\right)^3 \left(\frac{\sigma - \sigma_0}{G}\right)^2 , \quad (1)$$

where $\dot{\epsilon}$ is the strain rate, D_0 the pre-exponential constant for diffusivity, G the shear modulus, b the Burgers vector, k the Boltz-mann's constant, T the absolute temperature, R the gas constant, d the grain size, σ the flow stress, and σ_0 the threshold stress. For the present FSP Mg–Zn–Y–Zr, no threshold-type deformation behavior is expected because a constant strain rate sensitivity of ~0.5 was observed throughout the investigated strain rates of 3×10^{-4} to 1×10^{-2} s^{-1}. In Fig. 10, the superplastic data of the FSP Mg–Zn–Y–Zr were plotted as $\dot{\epsilon}kTd^3/D_gGb^4$ versus σ/G. For comparison, a straight line predicted by Eq. (1) and the superplastic data of ECAP AZ91, reported in Ref. 21, were also included. Figure 10 reveals three important observations. First, the temperature dependency of the superplastic flow for the FSP Mg–Zn–Y–Zr is similar to the activation energy for magnesium grain-boundary self-diffusion. Second, the normalized superplastic data of the FSP Mg–Zn–Y–Zr fit the straight line predicted by Eq. (1). Thus, Fig. 10 shows that grain boundary sliding is the main superplastic deformation mechanism for the FSP Mg–Zn–Y–Zr, and the superplastic data can be described by Eq. (1). Third, the superplastic deformation kinetics of this FSP Mg–Zn–Y–Zr is significantly faster than that of ECAP magnesium alloys under both as-ECAP and annealing conditions.

For the present study, although the FSP Mg–Zn–Y–Zr alloy did not exhibit enhanced superplastic deformation kinetics compared to the prediction by Eq. (1), the deformation kinetics of the FSP Mg–Zn–Y–Zr alloy is significantly faster than that of as-ECAP AZ91 alloy, which usually contains a great amount of non-equilibrium grain boundaries.[21] Even after a post-ECAP annealing that converts the non-equilibrium grain boundaries to the equilibrium ones, the deformation kinetics of the FSP Mg–Zn–Y–Zr alloy is still faster than that of the ECAP AZ91 alloy. This is accounted for by a complete recrystallized microstructure with a higher ratio of high-angle boundaries in the FSP Mg–Zn–Y–Zr alloy.

V. CONCLUSIONS

FSP resulted in significant breakup and dispersion of the coarse W-phase and remarkable grain refinement (~5.2 μm) in extruded Mg–Zn–Y–Zr alloy.

Maximum elongation of 635% was achieved at 450 °C and a relatively high strain rate of 3×10^{-3} s^{-1} with a strain-rate sensitivity of ~0.5 being observed at 400–450 °C for the strain rate of 3×10^{-4} to 1×10^{-2} s^{-1}.

An analysis of the superplastic data of the FSP Mg–Zn–Y–Zr revealed a stress exponent of two and

activation energy close to that for grain-boundary self-diffusion, suggesting that the grain boundary sliding is the primary deformation mechanism.

The superplastic deformation kinetics of the FSP Mg–Zn–Y–Zr is significantly faster than that of ECAP magnesium alloys.

ACKNOWLEDGMENTS

This work was supported by the National Outstanding Young Scientist Foundation for Z.Y. Ma under Grant No. 50525103, the National Basic Research Program of China under Grant No. 2006CB605205, and the Hundred Talents Program of Chinese Academy of Sciences.

REFERENCES

1. Y.Z. Lu, Q.D. Wang, W.J. Ding, X.Q. Zeng, and Y.P. Zhu: Fracture behavior of AZ91 magnesium alloy. *Mater. Lett.* **44,** 265 (2000).
2. G.M. Xie, Z.Y. Ma, L. Geng, and R.S. Chen: Microstructural evolution and mechanical properties of friction stir welded Mg–Zn–Y–Zr alloy. *Mater. Sci. Eng., A* **471,** 63 (2007).
3. Y. Kim and D. Bae: Superplasticity in a fine-grained Mg–Zn–Y–Zr alloy containing quasicrystalline particles. *Mater. Trans.* **45,** 3298 (2004).
4. M.Y. Zheng, S.W. Xu, K. Wu, S. Kamado, and Y. Kojima: Superplasticity of Mg-Zn-Y alloy containing quasicrystal phase processed by equal channel angular pressing. *Mater. Lett.* **61,** 4406 (2007).
5. W.M. Thomas, E.D. Nicholas, J.C. Needham, M.G. Murch, P. Templesmith, and C.J. Dawes: GB Patent Application No. 9125978.8, December 1991.
6. R.S. Mishra and Z.Y. Ma: Friction stir welding and processing. *Mater. Sci. Eng., R* **50,** 1 (2005).
7. Z.Y. Ma, R.S. Mishra, and M.W. Mahoney: Superplastic deformation behaviour of friction stir processed 7075 Al alloy. *Acta Mater.* **50,** 4419 (2002).
8. Z.Y. Ma, R.S. Mishra, M.W. Mahoney, and R. Grimes: Effect of friction stir processing on the kinetics of superplastic deformation in an Al–Mg–Zr alloy. *Metall. Mater. Trans. A* **36,** 1447 (2005).
9. P. Cavaliere and P.P. De Marco: Superplastic behaviour of friction stir processed AZ91 magnesium alloy produced by high pressure die cast. *J. Mater. Proc. Technol.* **184,** 77 (2007).
10. P. Cavaliere and P.P. De Marco: Friction stir processing of AM60B magnesium alloy sheets. *Mater. Sci. Eng., A* **462,** 393 (2007).
11. A.H. Feng and Z.Y. Ma: Enhanced mechanical properties of Mg–Al–Zn cast alloy via friction stir processing. *Scripta Mater.* **56,** 397 (2007).
12. J.A. Esparza, W.C. Davis, and L.E. Murr: Microstructure-property studies in friction-stir welded thixomolded magnesium alloy AM60. *J. Mater. Sci.* **38,** 941 (2003).
13. S.H.C. Park, Y.S. Sato, and H. Kokawa: Effect of micro-texture on fracture location in friction stir weld of Mg alloy AZ61 during tensile test. *Scripta Mater.* **49,** 161 (2003).
14. G.M. Xie, Z.Y. Ma, and L. Geng: Effect of microstructural evolution on mechanical properties of friction stir welded ZK60 alloy. *Mater. Sci. Eng., A* (in press).
15. Y. Zhang, X.Q. Zeng, L.F. Liu, C. Lu, H.T. Zhou, Q. Li, and Y.P. Zhu: Effects of yttrium on microstructure and mechanical properties of hot-extruded Mg–Zn–Y–Zr alloys. *Mater. Sci. Eng., A* **373,** 320 (2004).
16. J.Y. Lee, D.H. Kim, H.K. Lim, and D.H. Kim: Effects of Zn/Y ratio on microstructure and mechanical properties of Mg–Zn–Y–Zr alloys. *Mater. Lett.* **59,** 3801 (2005).
17. R.B. Figueiredo and T.G. Langdon: Development of superplastic ductilities and microstructural homogeneitiy in a magnesium ZK60 alloy processed by ECAP. *Mater. Sci. Eng., A* **430,** 151 (2006).
18. D.H. Bae, M.H. Lee, K.T. Kim, W.T. Kim, and D.H. Kim: Application of quasicrystalline particles as a strengthening phase in Mg–Zn–Y alloys. *J. Alloys Compd.* **342,** 445 (2002).
19. M.J. Stowell, D.W. Liversy, and N. Ridley: Cavity coalescence in superplastic deformation. *Acta Metall.* **32,** 35 (1984).
20. Z.Y. Ma and R.S. Mishra: Cavitation in superplastic 7075Al alloys prepared via friction stir processing. *Acta Mater.* **51,** 3551 (2003).
21. M. Mabuchi, K. Ameyama, H. Iwasaki, and K. Hiagshi: Low temperature superplasticity of AZ91 magnesium alloy with non-equilibrium grain boundaries. *Acta Mater.* **47,** 2047 (1999).
22. R.S. Mishra and M.W. Mahoney: Friction stir processing: A new grain refinement technique to achieve high strain rate superplasticity in commercial alloys. *Mater. Sci. Forum* **357–359,** 507 (2001).
23. A.F. Norman, I. Brough, and P.B. Prangnell: High resolution EBSD analysis of the grain structure in an AA2024 friction stir weld. *Mater. Sci. Forum* **331–337,** 1713 (2000).
24. I. Charit and R.S. Mishra: High strain rate superplasticity in a commercial 2024 Al alloy via friction stir processing. *Mater. Sci. Eng., A* **359,** 290 (2003).
25. T.G. Langdon: A unified approach to grain-boundary sliding in creep and superplasticity. *Acta Metall. Mater.* **42,** 2437 (1994).
26. H. Watanabe, H. Tsutsui, T. Mukai, and T. Aizawa: Realization of superplasticity in magnesium alloy and magnesium based composite. *Mater. Jpn.* **39,** 347 (2000).